ACS Photonics

Article

Cite This: ACS Photonics 2018, 5, 2200−2207

Tuning the Near-Infrared Absorption of Aromatic Amines on Tapered Fibers Sculptured with Gold Nanoparticles

Alina Karabchevsky,*[,†,‡,#] Aviad Katiyi,[†,‡,#] Muhammad Imran Mustafa Bin Abdul Khudus,[§] and Alexey V. Kavokin[∥,⊥]

[†]Electrooptical Engineering Unit, Ben-Gurion University of the Negev, Beer-Sheva 8410501, Israel

[‡]Ilse Katz Institute for Nanoscale Science and Technology, Ben-Gurion University of the Negev, Beer-Sheva 8410501, Israel

[#]Center for Quantum Information Science and Technology, Ben-Gurion University of the Negev, Beer-Sheva 8410501, Israel

[§]Photonics Research Centre, Department of Physics, Faculty of Science, University of Malaya, 50603 Kuala Lumpur, Malaysia

[∥]Department of Physics and Astronomy, University of Southampton, Southampton SO17 1BJ, U.K.

[⊥]CNR-SPIN, Viale del Politecnico 1, I-00133 Rome, Italy

Supporting Information

ABSTRACT: We discover an unexpected enhancement of the absorption of near-infrared light by aromatic amine overtones on photonic microfibers sculptured with gold nanoparticles. The adsorbed nanoparticles make the near-infrared spectroscopy of aromatic amines on microfibers feasible despite the small absorption cross-section of the molecular vibration overtones. We demonstrate that in the presence of gold nanomediators, the absorption of light by weak overtone transitions in *N*-methylaniline as a model analyte is dramatically enhanced. We attribute this effect to the increase of the mean trajectory of light in a microfiber due to its resonant scattering on metallic nanoparticles. The spectrally integrated transmittance scales with the concentration of nanoparticles to the power 1/6—the phenomenon of diffusive propagation of light. Practical applications of the discovered effect will include the detection of aromatic amines for efficient treatment of metabolic disorders resulting from the amino acids deficiency, research in biomedicine, and a number of bedside applications.

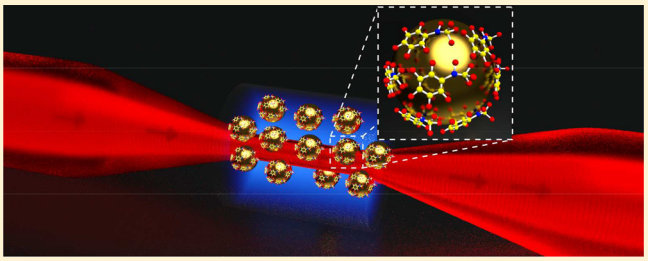

KEYWORDS: *Microfibers, diffusive propagation, N-methylaniline, nanoparticles, light-matter interaction, overtone spectroscopy, vibration spectroscopy*

Aromatic amines,[1,2] being the building blocks of aromatic amino acids, can be used to quantify the concentrations of essential proteins in natural products, functional materials, and plants.[3] The detection of these compounds is, therefore, a prominent topic in organic chemistry, with broad biomedical and industrial applications. One of the most straightforward and efficient approaches for detecting aromatic amines involves recording their fundamental vibrations in the mid-infrared (mid-IR) spectrum.[4−7] However, in practice, the cumbersome and costly equipment required to detect fundamental vibrations[7] hampers the facile application of this approach. A better solution lies in the near-infrared (NIR) region, since signatures of aromatic amines can also be deduced from the overtones (high harmonics of vibrational transitions) in NIR spectra.[8] NIR spectroscopy is a sensitive and affordable technique that is currently finding application in healthcare delivery, pharmaceuticals, neonatal and neurology (neurovascular coupling) research, and brain−computer interfaces. Nonetheless, the widespread implementation of NIR for the analysis of molecules is impeded by the fact that the cross-sections of vibrational transition overtones are orders of magnitude smaller than those of the corresponding fundamental transitions. Although the amine moiety of aromatic amines excited at around 1.5 μm was recently detected in a diffusive regime on planar glass waveguides[9] and on planar silicon nanostrip waveguides,[10] no attempts have been made to understand the mechanism of vibrational transitions of aromatic amines with broadband NIR illumination on surfaces of miniature guided wave devices, such as glass microfibers. This is not surprising, since the small absorption cross-section of vibrational transition overtones limits the use of conventional silica glass fibers. When embedded in media, with index close to that of the silica, fibers are optically weak guides. Therefore, the unmet need to develop a method for the surface spectroscopy of vibrational overtone transitions in the NIR region—a long-standing goal of molecular science—has attracted substantial research attention,[11,12] and to date several detection tools have been developed. These range from spectroscopy based on the plasmonic Fano resonances inherent in nanostructures, which gave improved molecular detection sensitivity when combined

Received: January 15, 2018
Published: March 29, 2018

DOI: 10.1021/acsphotonics.8b00025
ACS Photonics 2018, 5, 2200−2207

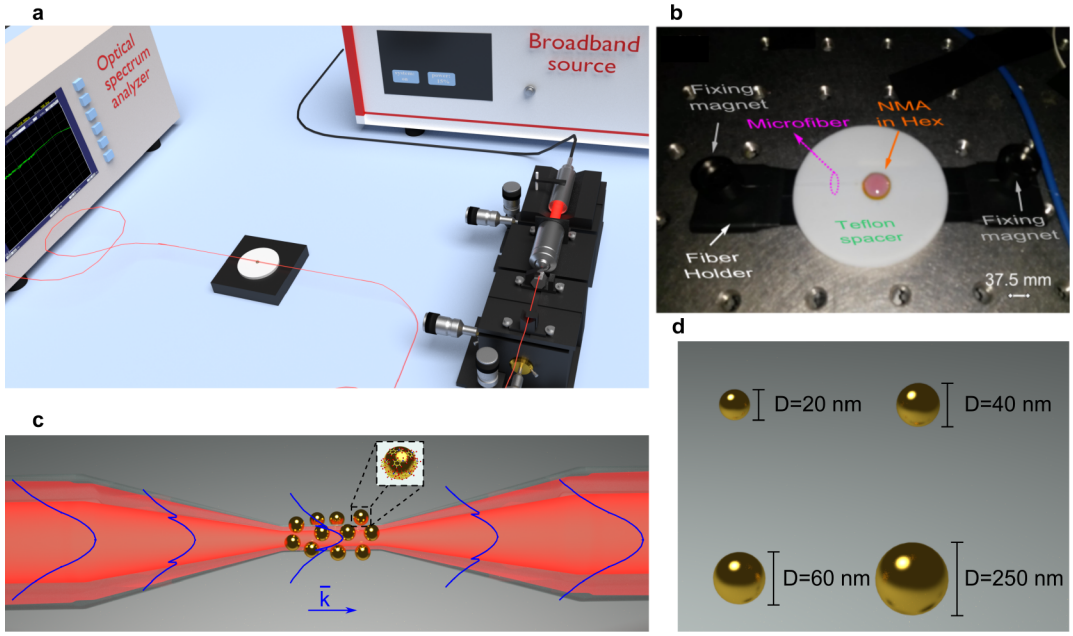

Figure 1. Experimental apparatus and sculptured microfiber architecture. (a) The experimental setup based on butt-coupled broadband illumination of a microfiber by a supercontinuum NIR source. The transmittance spectra are collected by an optical spectrum analyzer (see Methods). (b) Photograph of the microfiber fixed on the holder with magnets. A Teflon spacer protects the tapered region of the fiber from contamination by the holder. It also prevents the liquid from spreading out by virtue of the high surface tension of the Teflon. The labeling microfiber is pointing on the fiber which is transparent. (c) Schematic representation showing light guided in a glass microfiber sculptured with gold nanoparticles. (d) Schematic representation (not to scale) of the diameters of the nanoparticles used in the study. Note: the concentrations of nanoparticles are listed in Table S1 in the Supporting Information.

with surface enhanced coherent anti-Stokes Raman scattering (CARS),[13] to spectroscopy of vibrational overtones by single-molecule photodissociation.[14] However, the unknown impact on absorption both of the vibrational overtones from resonant Rayleigh scattering and of the diffusion of light in disordered media constitutes a critical obstacle to the efficient application of these methods. Recent advances in sensing applications in general, and particularly in spectroscopic applications, including techniques based on surface sensing, such as enhanced chemiluminescence,[15] surface-enhanced fluorescence spectroscopy,[16−18] Raman scattering spectroscopy,[13] and absorption spectroscopy,[7,19] rely on surface−medium interaction to enhance the effect of absorption and to improve the sensitivity beyond the standard spectroscopic limits.[12] However, the surface−medium interaction behavior of many important molecules, such as aromatic amines, remains unclear. It was this lack of vital knowledge, together with the strong potential applicability of molecular vibration spectroscopies in the detection of explosives and in the diagnostics of amine-based psychoactive stimulants and metabolic diseases, that motivated the present work.[2,19]

From the perspective of equipment miniaturization and portability, the guided-wave optics format is ideally suited to many applications that were traditionally based on free-space optics technology.[20] An additional advantage of this format lies in the low propagation losses compared to plasmonics.[21] Indeed, guided-wave optics as compared to the free-space optics is characterized by low propagation losses and large evanescent fields extending beyond the physical dimensions of the guiding layers. Note that a substantial amount of the transmitted power can be carried by the evanescent tail.[22] It was shown that the tapered ridge and microfiber structures exhibit an increased evanescent field, thus allowing for a strong interaction with the molecular layer and efficient probing of the overtones.[22] In addition, microfibers boast strong confinement, such that if the core dimensions of a microfiber are proportional to half the wavelength of the waveguide in it, the propagation beam is confined to fiber smallest waist dimensions, which gives rise to effects such as supercontinuum lasing, and nonlinear optical switching. Finally, microfibers are robust, with negligible surface roughness, which, in turn, translates into superior mechanical strength.[23] Guided-wave optics, therefore, enables the design and realization of compact surface sensors,[24,25] such as photonic waveguides[9,26,27] and microfibers.[23] The surface effect in these configurations is based on the evanescent tails of the guided mode. In the design of optical waveguides, the trade-off between miniaturization and guidance with high efficiency is aimed at enhanced interaction of electromagnetic radiation with the molecular medium for a guided modes as detailed in refs 22 and 28 Taken together, the above advantages have made guided-wave optics an important molecular spectroscopy tool. Guided-wave optics have been used as the basis for detecting overtone spectra in experimental studies of weak glass waveguides,[29] high refractive index contrast chalcogenide glass waveguides,[30] and high-Q factor silicon waveguide ring resonators.[31] Compared to planar waveguides, the micro- and nanofibers in miniaturized sensors are characterized by well-controlled evanescent fields, flexibility, configurability, high confinement, robustness, and compactness.[32] Microfibers are thus an excellent research tool and well suited to a wide range of applications, such as telecommunications, sensing,[33] optical manipulation[34] and high Q resonators, to list but a few.[23,35] Despite the clear benefits of using microfibers for molecular overtone absorption studies, this research tool remains unexploited.

DOI: 10.1021/acsphotonics.8b00025
ACS Photonics 2018, 5, 2200−2207

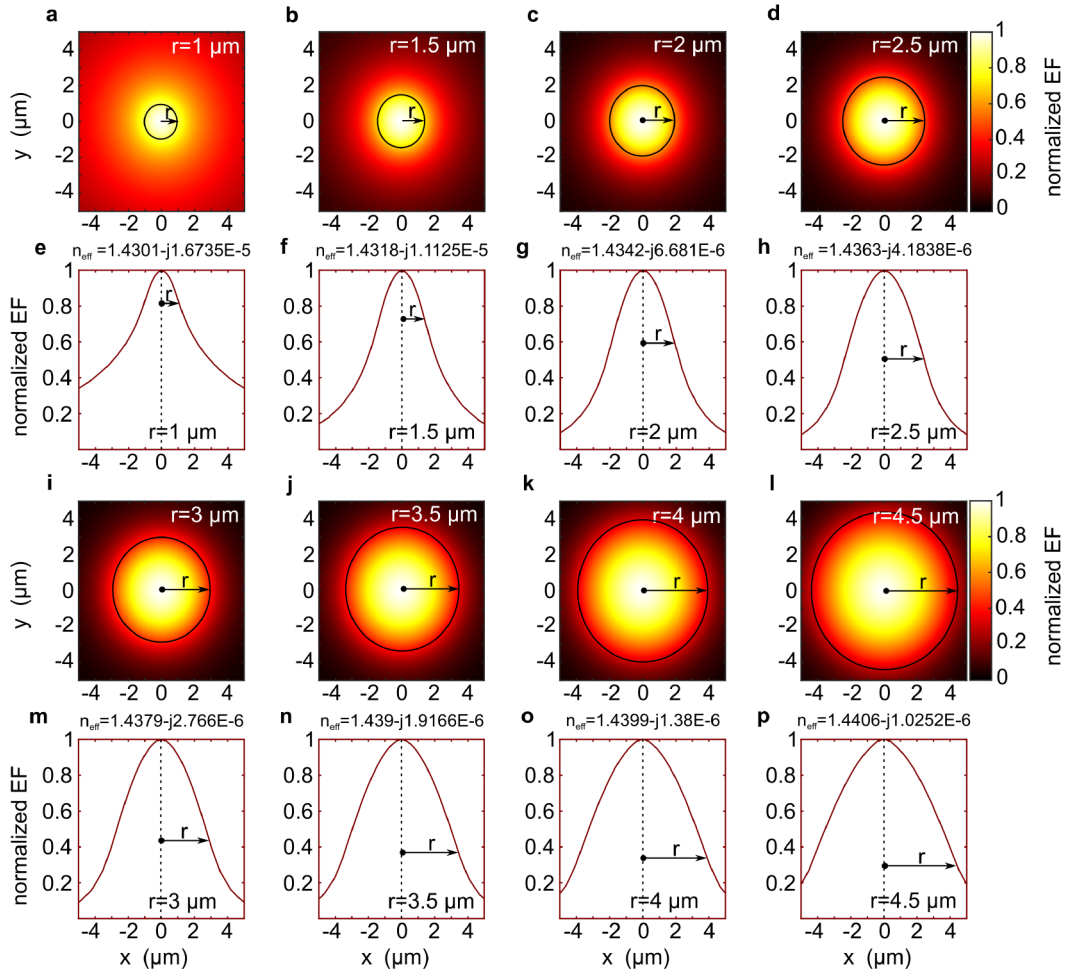

Figure 2. Numerical modeling. (a–d and i–l) Normalized electric field (EF) of microfibers, calculated according to eq 1, with various core radii embedded in NMA:hexane ratio 1:3. (e–h and m–p) Cross-sections at $y = 0$ μm.

RESULTS AND DISCUSSION

The motivation for the work is to study the mechanism of absorption by molecular vibrations overtones excited with evanescent fields in the NIR. For this, we combined several disciplines, namely, the physics of guided wave optics, the microfibers fabrication, the propagation of light in diffusive regime with nanoparticles, the surface chemistry, and the molecular overtone spectroscopy.

Here, we report the engineering of a guided wave tool utilizing microfibers sculptured with gold nanoparticles (previously studied as nanoamplifiers in opto-chemical reactions[15]) to study the absorption mechanism of molecular overtone vibrations. We show that in our system the overtone absorption depends primarily on the concentration of the nanoparticles on the microfiber, which electrostatically attract the probe molecule to the microfiber surface. We also show that the spectrally integrated transmittance scales with the concentration of nanoparticles to the power 1/6—a characteristic of the diffusive propagation of light, which is responsible for the enhanced resonant absorption.

In our experimental setup, collimated broadband light was focused onto the microfiber (Figure 1a). The light was then guided in the microfiber and collected in the optical spectrum analyzer. A Teflon spacer prevented contamination of the device. The low refractive index of the Teflon (1.3) relative to that of the silica fiber (1.43) at the NIR wavelengths of *N*-methylaniline (NMA) vibrations prevented leakage of the evanescent field. In Figure 1b, a photograph of the device shows that the fiber holder contained two magnets to fix the fiber in place and that a single droplet of the mixture of NMA in hexane was applied on the tapered region L of the microfiber above the Teflon spacer. Figure 1c is a schematic representation of the microfiber sculptured with gold nanoparticles, and Figure 1d shows the relative dimensions (not to scale) of the spherical nanoparticles that we used.

We found nontrivial broadband molecular overtone absorption in the NIR spectra on glass microfibers sculptured with gold nanoparticles. This effect allowed us to detect, for the first time, the broadband overtone absorption of the aromatic amine molecule NMA and to study the mechanism of overtone absorption on optically weak microfibers. Our proof-of-concept measurements showed that a compact NIR spectrometer based on a reconfigurable microfiber would have sufficient sensitivity and spectral resolution to facilitate the study of the fine electronic structure of a probe organic molecule. Pioneered by Akhlesh Lakhtakia, sculptured thin films have been used in variety of fundamental studies, for instance, for those of enhanced fluorescence with applications in biosensing.[16−18] Our method is based on the sculpturing of a microfiber with electronegative material such as gold nanoparticles. Nanoparticles (1) adsorb to the microfiber and (2) mediate the electrostatic attraction of amine-based molecules at the

DOI: 10.1021/acsphotonics.8b00025
ACS Photonics 2018, 5, 2200−2207

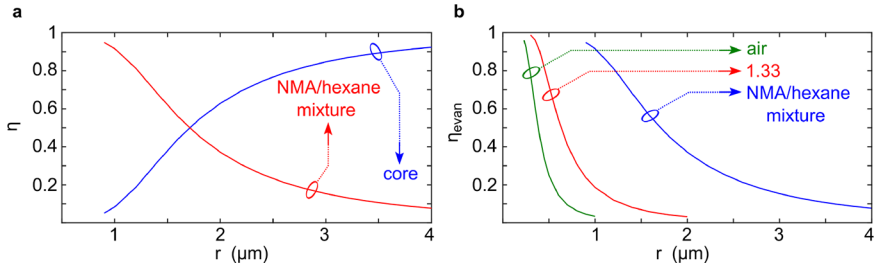

Figure 3. Numerical modeling. (a) The fraction of power in the core of the microfiber and in NMA:hexane (1:3) relative to the total power (see Methods). (b) Fraction of the power in the analyte η vs radius of a microfiber immersed in air, water, or a NMA:hexane mixture.

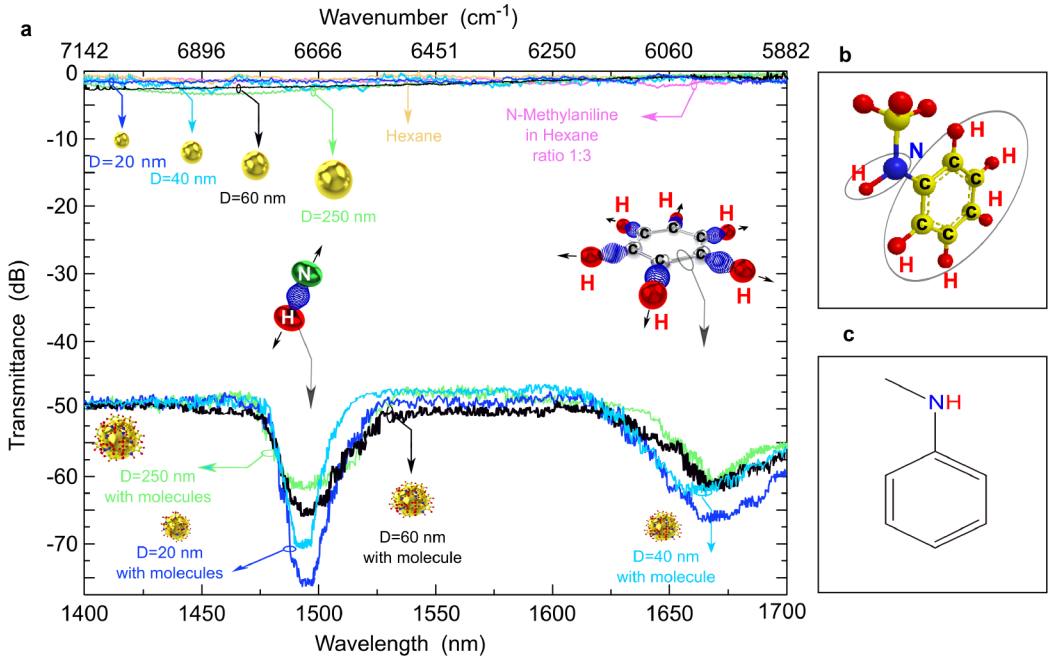

Figure 4. Measurement on the microfiber. (a) Transmittance spectra recorded on microfiber. NMA spectra detected on microfibers sculptured by different nanoparticles sizes show clear overtone absorption bands of (N−H)-bond stretching band around 1.5 μm and the aryl (C−H) overtone stretching band around 1.65 μm in the $\Delta V = 2$ region for NMA:hexane ratio 1:3. N−H and aryl C−H absorption bands are indicated by arrows; measured stretching motions of atomic bonds are indicated by springs. Upper curves represent the transmittance spectra of the microfiber embedded in the hexane, molecular mixture, and gold nanoparticles, respectively. Lower curves represent the transmittance spectra of the microfiber embedded in the molecular mixture together with the gold nanoparticles. (b) Chemical structure and (c) skeletal molecular shape of NMA.

nanoparticles, thereby contributing to disorder on the microfiber surface. As a result, the propagation of light in such a microfiber is strongly affected by the resonant Rayleigh scattering and therefore the mean trajectory of propagating photons becomes orders of magnitude longer in the resulting diffusive regime, as explained in the supplementary material of ref 9. Consequently, organic molecules are exposed to the passage of the light for a markedly longer time-a scenario that strongly augments the probability of absorption, which is crucial for the sensitivity of our evanescent-field-based research tool.

In our NMA:hexane system, diffusive propagation of the photon in the highly scattering medium slows down the light around the resonance of the overtone. The light-matter interaction enhancement is, therefore, due to the increased time τ that the photon spends in the medium, which leads to an increased mean trajectory L. The interaction between the photon and the analyte molecule thus continues for a longer time, resulting in enhanced absorption. This is not a result of the tapering routine. The tapering itself would not cause the slowing down of light on such a scale as in our experiments. The guided mode profile is different in the transition and tapered regions, which is a minor factor compared to the diffusive propagation of light due to the resonant Rayleigh scattering.[22,36] We note here that our system differs from the "conventional" plasmonics which is widely used to enhance light−matter interaction for sensing applications.[6] This enhancement derives from the excitation by light of free electrons at the metal−dielectric interface in noble metals when the momentum matching condition is fulfilled. Explicitly, the momentum of the incident photon must be equal to the momentum of the surface plasmon, resulting in the field effect. Excited surface plasmons facilitate field localization and field enhancement. Diffusive propagation of the photon in highly scattering medium of the molecules slows down the light around the resonance of the overtone. The enhancement here therefore, is due to the increased time the photon spent in the medium and resulting increased mean trajectory L as explained in details at supplementary section of ref 9. The fundamental reason for the NIR absorption induced by the microfiber sculptured with gold nanoparticles is the combination of chemical and physical effects, namely, (1) the chemical effect of

DOI: 10.1021/acsphotonics.8b00025
ACS Photonics 2018, 5, 2200−2207

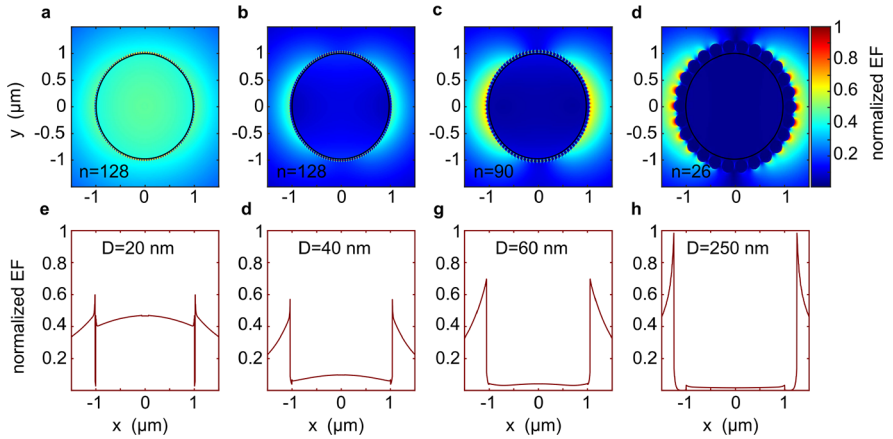

Figure 5. Numerical analysis. (a–d) Calculated normalized EF distributions for gold nanoparticles with D = 20, 40, 60, and 250 nm and maximal density without overlapping each other embedded in the molecular mixture. The corresponding cross-sections are shown in (e)–(h).

electrostatic adsorption: the adsorption of the nanoparticles to the microfiber surface results in the increased interaction between the molecules and the evenest wave of the fiber leading to the increased disorder in the system; (2) the physical effect of the diffusive propagation of light in the guiding mode: the quadrupole molecular moment induced by the evanescent field governs the scattering of light in the spectral vicinity of the overtone resonance absorption. The scattering causes the diffusive propagation of light that makes light spending a longer time in the absorbing medium.

In our system, as in other systems, the extent of the field distribution in a microfiber depends strongly on its core dimensions. Figure 2 shows that normalized electric field (EF) distribution colormaps and cross-sections all varied with the microfiber core radius, when the microfiber is embedded in NMA:hexane (ratio of 1:3). Normalized EF distributions were calculated using

$$\text{normalized EF} = \sqrt{\frac{E_x\ \text{conj}(E_x) + E_y\ \text{conj}(E_y) + E_z\ \text{conj}(E_z)}{\max[E_x\ \text{conj}(E_x) + E_y\ \text{conj}(E_y) + E_z\ \text{conj}(E_z)]}} \quad (1)$$

Figure 3a shows the dependence of microfiber radius on the fraction of the optical power in the core η, as defined in eq 5 in ref 22, and in the molecular medium ηm as defined in eq 4 in ref 22, illuminated by the evanescent field of the microfiber. A large fraction of the power extends into the medium of higher index, as shown in Figure 3a. For microfibers of r = 1 μm immersed in the analyte mixture, most of the light carried beyond the physical boundaries of the microfiber. Since more than 90% of the total power is carried in the evanescent tail (η > 0.9), such a system is ideal for sensing and detection. Figure 3b shows the change of the power fraction in the evanescent tail as a function of the microfiber radii immersed in air, water (refractive index of 1.33) or the NMA:hexane. The power starts to build up in the evanescent field at a microfiber radius of 2 μm or less. In this study, the microfiber had a core diameter of about 2 μm (1.8 μm), which potentially makes it favorable for sensing applications.[37] However, we found surprisingly the opposite to be the case. On a bare microfiber that had not been sculptured by gold nanoparticles there was no molecular signature observed in the NIR spectrum (upper spectrum in Figure 4a) in contrast to the spectra obtained on the microfibers sculptured with gold nanoparticles (lower part of Figure 4a). In the experiment reported here, a microfiber with 4 mm long tapered region, transmitted with the maximum loss of ~25 dB around the N–H vibration band of NMA (blue curve on Figure 4a).

In addition, our findings revealed a peculiar and unexpected dependence of the concentration of nanoparticles N, namely, the spectrally integrated transmittance scaled as $N^{1/6}$. Moreover, the 1/6 power law was shown to be a signature of the diffusive propagation of light in the presence of resonant scatters.[38] In our system, evidence for the diffusive propagation regime is the observed scaling of the integrated transmittance. Below we explain our experiments and present the corresponding analysis in detail.

A good estimate of the absorption $A(\lambda)$ as related to the transmittance $T(\lambda)$ may be expressed as $A(\lambda) \sim \log T(\lambda)$, (while neglecting a 4% Fresnel reflection) from the Beer–Lambert law:

$$T(\lambda) = -10 \log(e^{-4\pi L\kappa/\lambda}) \quad (2)$$

where the interaction of the molecules with the tapered region of the microfiber occurs along the distance L, and $\kappa(\lambda)$ is the extinction coefficient related to all nonradiative losses such as absorption losses $A(\lambda)$; $\kappa(\lambda)$ includes the scattering to waveguide modes, as given by

$$\kappa(\lambda) = \log_e[10^{A(\lambda)}]\frac{\lambda}{4\pi L} \quad (3)$$

According to the energy conservation law, the absorption spectrum of light in a fiber is related to the reflectivity R and the transmissivity T spectra as follows:

$$R(\lambda) + T(\lambda) + A(\lambda) = \text{const.} \quad (4)$$

From the experimental data, we deduce the spectral integral I of the absorption $A(\lambda)$, which is given by $I = WT(\lambda_p)$, where I is the product of the full width at half-maximum (fwhm) W and the depth of the transmission minimum at the molecular absorption line $T(\lambda_p)$. The fwhm is governed solely by the damping constant Γ_j of a vibrational band j from the dispersion function describing k vector dispersion of a multiple resonance Lorenz model dielectric.[29,39] The extinction coefficient presented in eq 2 is the imaginary part of the dispersion function: $\kappa(k) = \text{Im}\{\sqrt{\varepsilon(k)}\}$, with $\lambda = 1/k$. In this study, we calculated I for measured five tapered fibers that differed in

DOI: 10.1021/acsphotonics.8b00025
ACS Photonics 2018, 5, 2200–2207

terms of their respective concentrations of nanoparticles N and exciting molecular vibrations. Vibrational molecular absorption lines, which correspond to the changes in the vibrational state of the molecule, are governed by the intrinsic electronic structure of the molecule and essentially have no dependence on N. Nonetheless, here, a peculiar sublinear dependence $I \propto N^{\beta}$, where $\beta \approx 1/6$, was inaugurated, which is equivalent to the reported dependence on I of the propagation of exciton-polaritons in GaAs crystals with induced impurities.[40] Our observations indicate that light absorption was strongly amplified in our system due to light scattering by the organic molecules. The light remains in the fiber for a sufficiently long time to be absorbed with a high probability by molecules. This property will facilitate the realization of miniature spectrophotometers based on microfibers sculptured with nanoparticles. Figure 4a shows $T(\lambda)$ of the first overtone absorption region in the NIR spectrum of NMA:hexane mixtures. Stretching vibrational modes of the amine bond and C−H of aryl are indicated by springs.

In this study, we investigated the transmittance of light in a microfiber covered with gold nanoparticles in the presence of a mixture of NMA in hexane (Figure 5 and Supporting Information, Figures S3−S6). Our findings revealed that although for nanoparticles with diameter larger than D = 20 nm and fully covering the tapered region of the microfiber (Figure 5b−d vs Figure 5a) most of the light is within the molecular mixture, the device barely guides. Therefore, we would expect a higher signal for microfibers sculptured with gold nanoparticles of 20 nm diameter. The normalized EFs for different diameters of the gold nanoparticles were calculated based on eq 1. Normalized EF distributions (Figure 5a−d) and cross-sections (Figure 5e−h) showed marked discontinuity at the microfiber surface. In fibers, the lack of the radial symmetry arises from the boundary conditions for the axial and transversal components of the EF at the silica−molecular mixture boundary.[41] The optical mode is confined if the diameter of the nanoparticle is small, namely, D = 20 nm. However, for $D >$ 20 nm, a large fraction of the power interacts with the molecular mixture.

Any absorption by organics would intuitively be expected to scale linearly with N. Therefore, the observed dependence of the product I on N is a fascinating finding. A similar dependence of I on N was predicted for exciton-polaritons by Akhmediev,[42] which was theoretically traced,[43] and finally proved in a recent empirical work on exciton-polaritons propagating through thin crystal slabs.[40] It should be mentioned here that absorption by molecular overtone vibrations is an intrinsic property of molecules that is independent of the nanoparticle concentration N. However, the integrated absorption of light by molecules is dependent on the trajectory of the light and time it spends in the absorbing medium. Therefore, in view of the strong elastic scattering of NMA molecules, the effective trajectory of photons guided in the microfiber will become significantly longer than that in the ballistic regime, a scenario that indicates the "slow light" phenomenon.[9] The scattering by NMA and free carriers is expected to induce a switch in the propagation regime from ballistic to diffusive, as was previously demonstrated by us on channel waveguides made of glass.[9] Aromatic amines have a negative affinity to the glass base surfaces. Therefore, without surface treatment, detection of NMA with devices made of glass would not be possible. The sculpturing with gold nanoparticles is crucial as it provides the electrostatic adsorption of the NMA:hexane mixture molecules to the surface of gold. Below we show that the integrated absorption in the diffusive propagation regime is, in fact, powered by the characteristic time spent by the diffusing photons in the molecular layer and is related nonlinearly to the nanoparticle concentration N.

To describe the diffusive propagation of light in a microfiber, we assume that elastic scattering dominates the delay in photonic propagation, and we neglect any inelastic scattering by nanoparticles or acoustic phonons. The propagation of photons in a guide with a dense diffusive species which are NMA molecules can be characterized by the classical diffusion equation for the concentration of photons $n(\lambda,x,t)$ at wavelength λ, coordinate x, and time t:

$$\frac{\partial n(\lambda, x, t)}{\partial t} = D(\lambda)\frac{\partial^2 n(\lambda, x, t)}{\partial x^2} - \frac{n(\lambda, x, t)}{\tau(\lambda)} \tag{5}$$

where wavelength-dependent $D(\lambda)$ and $\tau(\lambda)$ are the diffusion coefficient and nonradiative photon lifetime, which are responsible for the absorption of light by NMA molecules, respectively.

The delay time due to diffusive photon propagation, $T_D(\lambda)$, can be found from the condition $\partial n(\lambda,L,t)/\partial t = 0$ (see ref 38 for details):

$$T_D(\lambda) = \sqrt{\left[\frac{\tau(\lambda)}{4}\right]^2 + \frac{L^2\tau(\lambda)}{4D(\lambda)}} - \frac{\tau(\lambda)}{4} \tag{6}$$

At the strong absorption limit, the photon nonradiative time is sufficiently short for $\tau(\lambda) \ll L^2/D(\lambda)$, where the delay is proportional to the sample thickness, as in the case of the ballistic propagation, $T_D(\lambda) = (L/2) \times\sqrt{\tau(\lambda)/D(\lambda)}$. The diffusion constant $D(\lambda) = v_g(\lambda)l(\lambda)/3$, where $v_g(\lambda)$ is the group velocity of the photon penetrating to the molecular layer covering the guide. The group velocity does not depend on the concentration of the nanoparticles. The photon mean free path is proportional to the average distance between the scattering centers, and, according to ref 40, $l(\lambda) \sim N^{-1/3}$. Consequently, at the strong absorption limit, the integrated absorption is expected to depend on the concentration of nanoparticles as

$$I \sim \int \frac{T_D(\omega)}{\tau(\omega)} \sim N^{1/6} \tag{7}$$

Figure 6 shows the integrated absorption as a function of the concentration of nanoparticles calculated using the diffusion

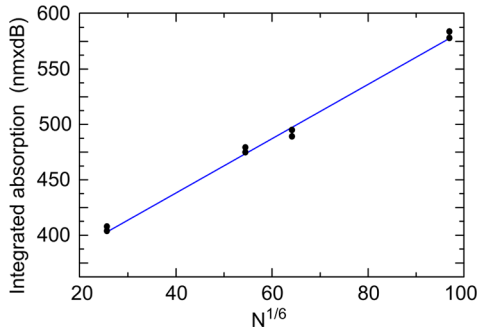

Figure 6. Integrated molecular absorption with the concentration of nanoparticles. Each experimental point represents a separate measurement on the different device. Straight line accounts for the prediction of the diffusive model from eq 7.

DOI: 10.1021/acsphotonics.8b00025
ACS Photonics 2018, 5, 2200−2207

model described above. It accurately reproduces our experimental observations and demonstrates the correct functional dependence between the integrated absorption and the concentration of the nanoparticles in a microfiber guide. This relationship confirms the diffusive mechanism of the amplification of the overtone absorption in a microfiber in the presence of nanoparticles.

The NIR absorption induced by the microfiber sculptured with gold nanoparticles may be attributed to a combination of chemical and physical effects, as follows: (1) the chemical effect of electrostatic adsorption of the nanoparticles on the microfiber surface promotes the interaction between the molecules and the evanescent wave of the fiber and increases disorder in the system; and (2) the physical effect of near fields is manifested in the NIR region by the evanescent field inducing molecular quadrupole moments (second moments), which contribute to the scattering of light around the overtone resonance absorption.

CONCLUSIONS

To conclude, the first broadband demonstration of overtone molecular signatures in the NIR spectrum was reported in a diffusive regime induced by metallic nanoparticles on silica tapered fibers. The mechanism of broadband NIR absorption by NMA overtones was explained in terms of the long nonradiative time of the photon guided in a microfiber sculptured with electronegative gold nanoparticles. Our system serves as a new design for reconfigurable microfiber sensors, potentially allowing aromatic amines to be identified by broadband NIR transmission spectroscopy. The maximum enhancement of the absorption is scaled with the concentration of nanospheres to the power 1/6. The reconfigurable microfiber system allows for the broadband detection of molecular signatures in the NIR spectral range with a high precision. The Purcell effect triggered by metallic nanoparticles is not observed here. If present, it would contribute with a linear dependence of the integrated absorption on N that would be easy to extract. However, we clearly see a much weaker dependence that is excellently described by the $N^{1/6}$ dependence. The diffusive theory described in the paper as applied to the propagation of polaritons can be directly generalized to describe the observed Fano resonances in terms of the diffusive propagation of plasmonic excitations. We have opted for using the simplified ray optics model due to its utmost simplicity and the advantage of yielding the analytical results. The description in terms of plasmon diffusion is possible but would be cumbersome, as we work very far from the plasmon resonances in gold nanoparticles, and the frequencies of the plasmon modes in our system are strongly distributed due to the size dispersion of gold nanoparticles.

The sculptured microfiber approach, giving a disorder-enhanced vibrational absorption effect, can also be applied for straightforward measurements of other physical entities such as magnetic field and ionization radiation. Overtone molecular vibrations can be detected remotely through guided modes.

METHODS

We fabricated the microfibers by tapering conventional SMF-28 fibers. The core diameter of the fiber before tapering was 8.5 μm and cladding diameter was about 127 μm. We used the tapering procedure based on the modified flame brushing technique,[22,23] in which a microheater was used to heat the fiber locally toward its softening point. Once heated, the microfiber was pulled longitudinally with microstages to reduce its diameter. Eventually, the cladding replaced the original core of the microfiber, thereby producing a tapered region of 2 μm in diameter, which consisted solely of the cladding material. Therefore, we used the tapered microfiber as a guided wave analytical tool and the analyte solution became the new cladding. We minimized the losses of microfiber material by accurate modeling of the microfiber profile, as detailed in ref.[44] We conducted the optical microfiber measurements of transmittance spectra using the apparatus shown in Figure 1a. NIR light was generated by a high-power supercontinuum fiber source (Fianium SC-600-FC) operating at a central wavelength of 1060 nm, with a spectral bandwidth spanning 450 nm to >1750 nm and generating optical pulses of less than 10 ps in duration. We collimated and focused the broadband light onto the microfiber using an objective NA of 0.25 and ×10 magnification. The power transmitted through the microfiber was collected while the microfiber was coupled directly into an optical spectrum analyzer (OSA, Yokogawa AQ6370). Spectral resolution was set at 0.5 nm. The acquisition time for the 300 nm spectral window was about 50 s. No polarization dependency was observed. The refractive index of pure aromatic amine NMA is 1.57118, which is much higher compared to the index of silica fibers. Therefore, the refractive index of NMA was reduced by diluting the amine with hexane, having a refractive index of 1.37508, to a ratio of 1:3 NMA:hexane. The refractive indexes of the liquids were measured with an RA 510 refractometer operating at 589 nm at a room temperature of 21 ± 2 °C. The microfibers were modeled using COMSOL Multiphysics 5 available at the Light-on-a-Chip group (Ben-Gurion University of the Negev). Since the effect of the doped silica core vanishes at microfiber diameters a few times the wavelength, the cladding of the original fiber was assumed to be the new core and the new cladding to be air or the NMA in hexane mixture. Therefore, to explore theoretically the modes propagating in the microfiber waist, a two-layer system was adapted for microfibers of 2 μm in diameter and less.[37] The first layer is the silica core having a refractive index of 1.44; this layer is surrounded by air or the NMA:hexane mixture.

ASSOCIATED CONTENT

Supporting Information

The Supporting Information is available free of charge on the ACS Publications website at DOI: 10.1021/acsphotonics.8b00025.

NIR spectra of NMA and hexane; summary of number and integrated absorption of gold particles of different diameters; normalized EF images and cross-sections; normalized EF colormaps for microfibers with varying nanoparticle densities and diameters (PDF)

AUTHOR INFORMATION

Corresponding Author

*E-mail: alinak@bgu.ac.il.

ORCID

Alina Karabchevsky: 0000-0002-4338-349X

Aviad Katiyi: 0000-0002-7924-9065

Notes

The authors declare no competing financial interest.

DOI: 10.1021/acsphotonics.8b00025
ACS Photonics 2018, 5, 2200−2207

■ ACKNOWLEDGMENTS

The authors acknowledge the support of the Multidisciplinary Program Health-Engineering Sciences grant by the Ben-Gurion University of the Negev. The authors thank Prof. Ohad Medalia (BGU) for consultation on the surface treatment and Dr. Avi Niv for kindly lending the supercontinuum light source to perform the measurements.

■ REFERENCES

(1) Peeks, M. D.; Claridge, T. D.; Anderson, H. L. Aromatic and antiaromatic ring currents in a molecular nanoring. *Nature* **2017**, *541*, 200−203.
(2) Salvatore, R. N.; Yoon, C. H.; Jung, K. W. Synthesis of secondary amines. *Tetrahedron* **2001**, *57*, 7785−7811.
(3) Tzin, V.; Galili, G. The biosynthetic pathways for shikimate and aromatic amino acids in Arabidopsis thaliana. *Arabidopsis Book* **2010**, *8*, e0132.
(4) Lecaplain, C.; Javerzac-Galy, C.; Gorodetsky, M.; Kippenberg, T. Mid-infrared ultra-high-Q resonators based on fluoride crystalline materials. *Nat. Commun.* **2016**, *7*, 13383.
(5) Lanin, A.; Voronin, A.; Fedotov, A.; Zheltikov, A. Time-domain spectroscopy in the mid-infrared. *Sci. Rep.* **2015**, *4*, 6670.
(6) Stanley, R. Plasmonics in the mid-infrared. *Nat. Photonics* **2012**, *6*, 409−411.
(7) Li, Y.; Su, L.; Yu, C.; Deng, J.; Fang, Y.; Shou, C. Surface-enhanced molecular spectroscopy (SEMS) based on perfect-absorber metamaterials in the mid-infrared. *Sci. Rep.* **2013**, *3*, 2865.
(8) Skumanich, A.; Moylan, C. R. The vibrational overtone spectrum of a thin polymer film. *Chem. Phys. Lett.* **1990**, *174*, 139−144.
(9) Karabchevsky, A.; Kavokin, A. Giant absorption of light by molecular vibrations on a chip. *Sci. Rep.* **2016**, *6*, 21201.
(10) Katiyi, A.; Karabchevsky, A. Si Nanostrip Optical Waveguide for On-Chip Broadband Molecular Overtone Spectroscopy in Near-Infrared. *ACS Sensors* **2018**, *3*, 618.
(11) Bernhardt, B.; Ozawa, A.; Jacquet, P.; Jacquey, M.; Kobayashi, Y.; Udem, T.; Holzwarth, R.; Guelachvili, G.; Hänsch, T. W.; Picqué, N. Cavity-enhanced dual-comb spectroscopy. *Nat. Photonics* **2010**, *4*, 55−57.
(12) Banwell, C.; McCash, E. M. *Fundamentals of Molecular Spectroscopy*; McGraw-Hill, 1994; p 85.
(13) Zhang, Y.; Zhen, Y.-R.; Neumann, O.; Day, J. K.; Nordlander, P.; Halas, N. J. Coherent anti-Stokes Raman scattering with single-molecule sensitivity using a plasmonic Fano resonance. *Nat. Commun.* **2014**, *5*, 4424.
(14) Khanyile, N. B.; Shu, G.; Brown, K. R. Observation of vibrational overtones by single-molecule resonant photodissociation. *Nat. Commun.* **2015**, *6*, 7825.
(15) Karabchevsky, A.; Mosayyebi, A.; Kavokin, A. V. Tuning the chemiluminescence of a luminol flow using plasmonic nanoparticles. *Light: Sci. Appl.* **2016**, *5*, e16164.
(16) Liebermann, T.; Knoll, W. Surface-plasmon field-enhanced fluorescence spectroscopy. Colloids and Surfaces A: *Colloids Surf., A* **2000**, *171*, 115−130.
(17) Abdulhalim, I.; Karabchevsky, A.; Patzig, C.; Rauschenbach, B.; Fuhrmann, B.; Eltzov, E.; Marks, R.; Xu, J.; Zhang, F.; Lakhtakia, A. Surface-enhanced fluorescence from metal sculptured thin films with application to biosensing in water. *Appl. Phys. Lett.* **2009**, *94*, 063106.
(18) Karabchevsky, A.; Patzig, C.; Rauschenbach, B.; Abdulhalim, I. Microspot surface enhanced fluorescence from sculptured thin films for control of antibody immobilization. *Proc. SPIE* **2011**, 81040L.
(19) Abb, M.; Wang, Y.; Papasimakis, N.; De Groot, C.; Muskens, O. L. Surface-enhanced infrared spectroscopy using metal oxide plasmonic antenna arrays. *Nano Lett.* **2014**, *14*, 346−352.
(20) Midwinter, J. Trends in optical fibre transmission research. *Nature* **1976**, *261*, 371−376.
(21) Maier, S. A. *Plasmonics: fundamentals and applications*; Springer Science & Business Media, 2007.
(22) Katiyi, A.; Karabchevsky, A. Figure of merit of all-dielectric waveguide structures for absorption overtone spectroscopy. *J. Lightwave Technol.* **2017**, *35*, 2902−2908.
(23) Brambilla, G. Optical fibre nanowires and microwires: a review. *J. Opt.* **2010**, *12*, 043001.
(24) Ash, E.; Pitt, C.; Wilson, M. Integrated optical circuits for telecommunications. *Nature* **1976**, *261*, 377−381.
(25) Midwinter, J. On the use of optical waveguide techniques for internal reflection spectroscopy. *IEEE J. Quantum Electron.* **1971**, *7*, 339−344.
(26) Hua, P.; Hole, J. P.; Wilkinson, J. S.; Proll, G.; Tschmelak, J.; Gauglitz, G.; Jackson, M. A.; Nudd, R.; Griffith, H. M.; Abuknesha, R. A.; Kaiser, J.; Kraemmer, P. Integrated optical fluorescence multisensor for water pollution. *Opt. Express* **2005**, *13*, 1124−1130.
(27) Hua, P.; Luff, B. J.; Quigley, G. R.; Wilkinson, J. S.; Kawaguchi, K. Integrated optical dual Mach−Zehnder interferometer sensor. Sensors and Actuators B. *Sens. Actuators, B* **2002**, *87*, 250−257.
(28) Schwarz, B.; Reininger, P.; Ristanić, D.; Detz, H.; Andrews, A. M.; Schrenk, W.; Strasser, G. Monolithically integrated mid-infrared lab-on-a-chip using plasmonics and quantum cascade structures. *Nat. Commun.* **2014**, *5*, 4085.
(29) Karabchevsky, A.; Shalabney, A. Strong interaction of molecular vibrational overtones with near-guided surface plasmon polariton. *Proc. SPIE* **2016**, 98991T−1.
(30) Hu, J.; Tarasov, V.; Agarwal, A.; Kimerling, L.; Carlie, N.; Petit, L.; Richardson, K. Fabrication and testing of planar chalcogenide waveguide integrated microfluidic sensor. *Opt. Express* **2007**, *15*, 2307−2314.
(31) Nitkowski, A.; Chen, L.; Lipson, M. Cavity-enhanced on-chip absorption spectroscopy using microring resonators. *Opt. Express* **2008**, *16*, 11930−11936.
(32) Tong, L.; Gattass, R. R.; Ashcom, J. B.; He, S.; Lou, J.; Shen, M.; Maxwell, I.; Mazur, E. Subwavelength-diameter silica wires for low-loss optical wave guiding. *Nature* **2003**, *426*, 816−819.
(33) Peterson, J. I.; Vurek, G. G. Fiber-optic sensors for biomedical applications. *Science* **1984**, *224*, 123−128.
(34) Grier, D. G. A revolution in optical manipulation. *Nature* **2003**, *424*, 810−816.
(35) Schwelb, O. Transmission, group delay, and dispersion in single-ring optical resonators and add/drop filters-a tutorial overview. *J. Lightwave Technol.* **2004**, *22*, 1380−1394.
(36) Marcuse, D. *Light transmission optics*; Van Nostrand Reinhold, 1972.
(37) Ismaeel, R. Microfiber devices based on evanescent field coupling. Ph.D. thesis, University of Southampton, 2015.
(38) Shubina, T.; Glazov, M.; Toropov, A.; Gippius, N.; Vasson, A.; Leymarie, J.; Kavokin, A.; Usui, A.; Bergman, J.; Pozina, G.; Monemar, B. Resonant light delay in GaN with ballistic and diffusive propagation. *Phys. Rev. Lett.* **2008**, *100*, 087402.
(39) Oughstun, K. E.; Cartwright, N. A. On the Lorentz-Lorenz formula and the Lorentz model of dielectric dispersion. *Opt. Express* **2003**, *11*, 1541−1546.
(40) Zaitsev, D.; Il'ynskaya, N.; Koudinov, A.; Poletaev, N.; Nikitina, E.; Egorov, A. Y.; Kavokin, A.; Seisyan, R. Diffusive propagation of exciton-polaritons through thin crystal slabs. *Sci. Rep.* **2015**, *5*, 11474.
(41) Okamoto, K. *Fundamentals of optical waveguides*; Academic Press, 2010.
(42) Akhmediev, N. Role of spatial dispersion in light absorption by excitons. *Zh. Eksp. Teor. Fiz.* **1980**, *79*, 1534−1543.
(43) Averkiev, N.; Savchenko, G.; Seisyan, R. Elastic scattering of exciton polaritons. *Phys. Solid State* **2015**, *57*, 290−295.
(44) Birks, T. A.; Li, Y. W. The shape of fiber tapers. *J. Lightwave Technol.* **1992**, *10*, 432−438.

DOI: 10.1021/acsphotonics.8b00025
ACS Photonics 2018, 5, 2200−2207